Digital post-processing for reducing A/D converter nonlinear distortion in wideband radio receivers

Digital Post-Processing for Reducing A/D Converter Nonlinear Distortion in Wideband Radio Receivers

Markus Allén, Jaakko Marttila and Mikko Valkama
Department of Communications Engineering
Tampere University of Technology
P.O. Box 553, FI-33101, Tampere, FINLAND
markus.allen@tut.fi, jaakko.marttila@tut.fi, mikko.e.valkama@tut.fi

***Abstract*—This article addresses the reduction of analog-to-digital (A/D) converter nonlinearities in radio receivers using digital signal processing (DSP). The main focus is on wideband A/D conversion where a collection of different waveforms at different frequency channels is digitized as a whole. The overall dynamic range in such composite signal can easily be in the order of tens of dB's, especially in the emerging cognitive radio type developments, and the nonlinear distortion due to strong carriers can easily block the weaker signal bands. In this article, DSP-based post-processing is proposed and demonstrated for reducing the effects of A/D converter integral nonlinearities (INL), stemming from unintentional deviations in the quantization intervals, as well as clipping due to improper input conditioning in wideband radio receiver context.**

Keywords-A/D converter; radio receiver; nonlinear distortion; integral nonlinearity; clipping; interference cancellation

I. INTRODUCTION

One of the main trends in designing and implementing radio transmitters and receivers for different wireless systems is to implement more and more of the transceiver functionalities using DSP [1]. In such transceiver implementations, especially on the receiver side, the performance of the A/D interface can easily become of a limiting factor to the whole receiver performance, particularly in cases where the dynamic range of the digitized waveform is high [2]-[5]. One fundamental issue is the inherent trade-off between resolution (number of bits) and speed (sampling rate), which is fairly well understood in the existing literature [6]-[8]. Other important issues in radio receiver context are signal distortion due to sampling jitter and A/D converter nonlinearities [2]-[8].

In this article, we focus on the A/D converter nonlinearity aspects. This is becoming an increasingly important issue in the emerging wireless systems, like IMT-Advanced [9], in which the spectrum allocation of individual terminals can be strongly scattered over a wide range of frequencies. In such cases, and also in more traditional radio systems in which most of the selectivity filtering in the terminal is implemented using DSP, the dynamic range of the digitized signal can be tens of dB's (even 50-60 dB). Similar or even more challenging input conditions are also expected in the emerging cognitive radio type developments where the available spectrum chunks can be heavily scattered over several hundreds of MHz total bandwidth. In this kind of scenarios, any nonlinearities in the A/D converter can cause severe intermodulation distortion (IMD) due to strong incoming signals which can easily block the weak desired signal bands [3]-[5]. Practical sources of nonlinearities in A/D converters are, e.g., integral and differential nonlinearity (INL and DNL) stemming from the unintentional deviations in the consecutive quantization levels, and clipping type distortion due to improper input signal conditioning (crossing the converter full scale voltage range).

Correction of A/D converter nonidealities has generally been studied rather widely in the literature, see, e.g., [2], [6], [10] and the references therein. Typical post-processing solutions are based on either look-up table methods or black-box modeling and identification type approaches. Most of these methods require specific off-line calibration signals and are thus mainly designed for measurement and instrumentation purposes in which the operating environment is typically very stable. On the radio terminal side, on the other hand, the operating conditions of the used electronics components as well as also the received waveform characteristics can both be easily heavily time-varying, implying that off-line calibration based approaches are not directly applicable. In this article, building on proper nonlinearity modeling, on-line DSP-based post-processing for reducing the intermodulation distortion in wideband A/D converters is proposed. Adaptive filtering based approach utilizing adaptive interference cancellation (AIC) is deployed and demonstrated to be able to considerably reduce the effects of INL and clipping at the weak desired signal bands in wideband radios. Compared to the existing literature, the proposed approach has the benefit of being able to tune the correction capabilities on a received packet-by-packet basis to the most sensitive (weak) parts of the received spectrum. This is seen very critical in the emerging future cognitive radio type developments.

II. A/D CONVERTER NONLINEARITIES IN RADIOS

In an ideal quantizer, based on the number of bits B, the overall full scale (FS) voltage range of the converter is uniformly divided into quantization levels. This is illustrated in Fig. 1. One source of nonlinear distortion, other than ordinary

This work was supported by the Academy of Finland (under the project "Understanding and Mitigation of Analog RF Impairments in Multiantenna Transmission Systems"), the Finnish Funding Agency for Technology and Innovation (Tekes, under the project "Advanced Techniques for RF Impairment Mitigation in Future Wireless Radio Systems") and the Technology Industries of Finland Centennial Foundation.

uniform quantization noise, is then coming from *unintentional deviations of the quantization levels* from the nominal ones [6], [10], [13]. This can be further divided into differential nonlinearity (DNL) and integral nonlinearity (INL). DNL refers to the differences in the actual codewidths (relative to ideal codewidth) while INL refers to the corresponding differences in consecutive quantization thresholds. Mathematically these are given by [6], [13]

$$DNL(k) = \frac{Q_{true}(k) - Q}{Q} \tag{1}$$

and

$$INL(k) = \frac{T_{true}(k) - T(k)}{Q} \tag{2}$$

where Q denotes the nominal quantization step (code width), k is the output code index and $T(k)$ denotes the nominal quantization threshold for code k. While DNL characteristics from output code to another can be typically fairly random, the INL behavior can have more deterministic shape [6], [10]. An example of typical INL as a function of the converter output code is given in Fig. 2.

Another clear source of nonlinear distortion is related to the *input signal conditioning* of the incoming signal relative to the converter full scale voltage FS. Any input dynamics exceeding the FS voltage range will essentially be *clipped* by the quantizer, i.e.,

$$k = \begin{cases} 0 & \forall x_{\mathrm{IN}} \le Q/2 \\ 2^{B-1} & \forall x_{\mathrm{IN}} > x_{\mathrm{FS}} - 3Q/2 \end{cases} \tag{3}$$

where x_{IN} denotes the converter input voltage and a FS voltage range of $0 \ldots x_{FS}$ is assumed. This is also illustrated in Fig. 1.

In radio receivers, both DNL and INL as well as clipping will cause intermodulation distortion [3], [6], [7], [11]. The dominant part of such distortion or spurious components is stemming from the deterministic INL behavior and also from possible clipping. Here both of these are essentially modeled using polynomial modeling of the form

$$\begin{aligned} x'_{\mathrm{IN}} &= g(x_{\mathrm{IN}}) \\ &= a_0 + a_1 x_{\mathrm{IN}} + a_2 x_{\mathrm{IN}}^2 + a_3 x_{\mathrm{IN}}^3 + \ldots \end{aligned} \tag{4}$$

which is then followed by an ideal quantizer. This is illustrated in Fig. 3 and is a fairly established modeling approach in the literature, see, e.g., [6], [10]-[12]. Typically the 2nd, 3rd, 5th and 7th order components are the most dominant ones. In case of clipping, fixed-order polynomial approximations (with odd orders) apply only within a given finite input dynamics [11]. For more details on clipping modeling with bandpass signals, refer to [14].

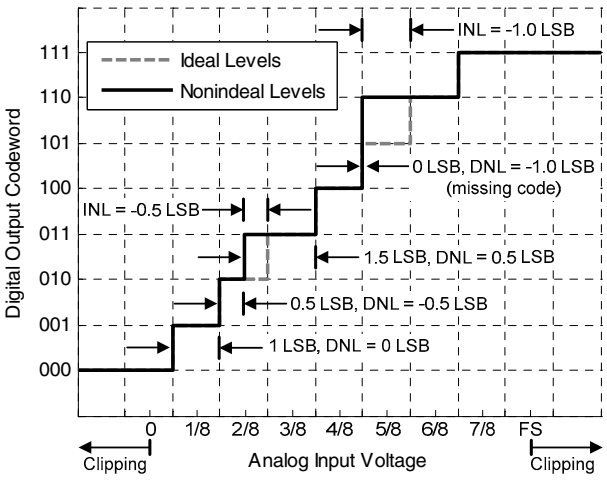

Fig. 1. Principal illustration of ideal and nonideal quantization with $B = 3$ bits. Both differential and integral nonlinearities (DNL, INL) as well as clipping are shown.

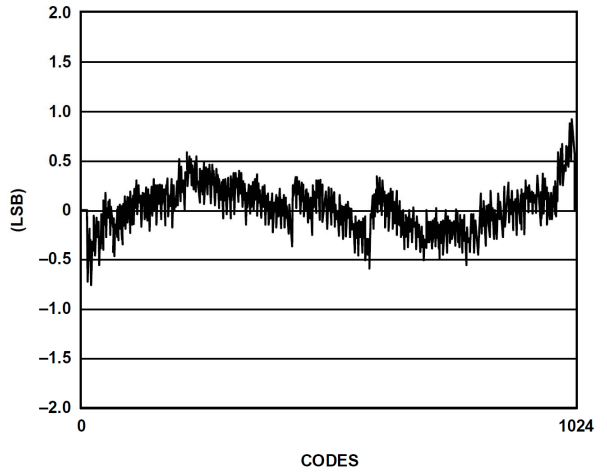

Fig. 2. Measured INL characteristics of 10-bit A/D converter AD9218 [17] as a function of output code k.

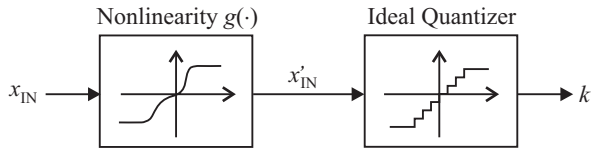

Fig. 3. Modeling A/D converter nonlinearities as a cascade of a memoryless polynomial followed by an ideal quantizer.

III. Digital Post-Processing

In this Section, stemming partially from the earlier studies related to receiver mixer and low noise amplifier (LNA) nonlinearities in [15] and [16], an adaptive interference cancellation based post-processing method is proposed for removing the intermodulation distortion due to A/D converter nonlinearities from the weak signal bands. A conceptual block-diagram is given in Fig. 4. First band-split filtering is applied to a block of digitized samples such that the most sensitive (weak) signal bands are isolated from the rest of the sampled signal spectrum (including the strong blocking signals). Then, for a given weak signal band, the interfering IMD frequencies are regenerated using polynomial signal processing and filtered using an adaptive filter whose output(s) are subtracted from the weak signal band. The coefficients of the adaptive filter stage are

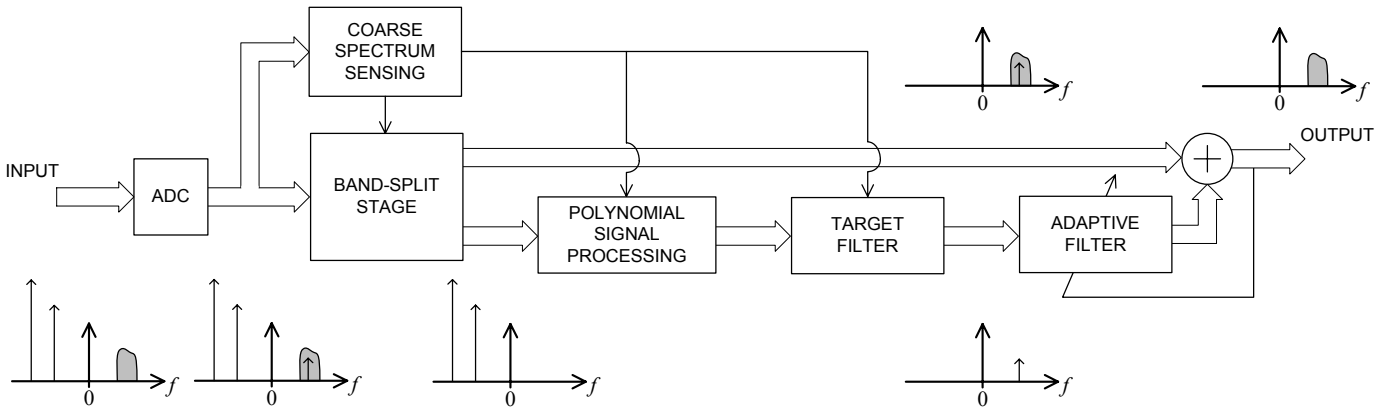

Fig. 4. Adaptive interference cancellation based digital post-processing scheme to reduce A/D converter nonlinear distortion at a weak signal band originating from strong blocking signals. In above, only a single IMD frequency is depicted on top of the weak signal for illustration purposes.

controlled such that the interference power at the weak signal band is minimized. The characteristics of the polynomial signal processing block, in turn, depend directly on the order of the IMD components being cancelled. In practice, different order IMD components can be processed either in parallel or serial manner, depending on the amount of computational resources, each having its own adaptive filter coefficients.

The overall coefficient adaptation, degrees of IMD being cancelled as well as the design of the band-split filtering stage can be controlled on a received packet-by-packet basis using an outer-loop control mechanism. This can be done based on coarse measurements of the spectrum density of the received packet using, e.g., FFT. Based on this spectrum sensing, the band-split filter characteristics are first tuned to isolate the most sensitive signal bands. Furthermore sensing the locations of the strongest signal energy levels (relative to the weak bands) gives the basis for choosing the IMD orders being cancelled. After this outer loop processing, the actual adaptive filter coefficients are controlled using e.g. the well-known least-mean-square (LMS) algorithm to minimize the IMD power at the overall output signal. These will be demonstrated in the following.

IV. Examples and Obtained Results

In this Section, practical examples are given to demonstrate the applicability of the proposed post-processing concept. Both INL as well as clipping effects are demonstrated and commercially available A/D converters are used in the experiments, covering both simulated as well as measured data.

A. Simulation Experiment for INL Reduction

Here a 10-bit off-the-shelf A/D converter [17] is experimented whose INL characteristics are shown in Fig. 2. An example received waveform consisting of 5 frequency channels with different channel bandwidths and power levels is deployed whose spectrum is illustrated in Fig. 5. The overall dynamic range in this experiment is in the order of 60 dB. The A/D converter sampling frequency is 32 MHz (both I and Q rails) and a converter model [18] provided by the component vendor is deployed in the simulations. In this example, 3rd order IMD of the strongest signal located at around -1 MHz is falling on top of the weak signal located at 3 MHz due to the INL. Example demodulated signal constellations without and with proposed digital post-processing are illustrated in the lower part of Fig. 5 for the weak QPSK signal located at 3 MHz. In the post-processing implementation, plain cubic operators are used as the polynomial signal processing blocks, independently for both I and Q branches, to regenerate the interfering IMD frequencies. Furthermore, independent single-tap adaptive filters are used then to weight and subtract the IMD estimates from the weak signal band. The well-known LMS algorithm is used in adaptive filter implementation with an adaptation block size of 5,000 samples. Clearly the proposed processing is able to reduce the intermodulation distortion effects considerably at the weak signal band.

B. Clipping Mitigation Using Measured Signals

Next the case of waveform clipping due to improper A/D converter input conditioning is demonstrated. Here realistic radio signal laboratory measurements combined with true-world 14-bit commercial A/D converter board [19] are used, instead of computer simulations, to emphasize practicality. For simplicity, 2 channel input waveform is used whose spectrum is illustrated in Fig. 6 together with the actual time-domain waveform characteristics. The used sampling frequency is 16 MHz for the I and Q rails. State-of-the-art laboratory signal generators are deployed to generate the measurement waveforms, and blocks of the digitized I and Q signals are stored into memory and loaded into PC for post-processing implementation.

Due to clipping, part of the energy of the strong signal at -1 MHz is falling on top of the weaker signal located at 3 MHz, which is again a QPSK signal. The digitized signal is next processed using the proposed post-processing targeting to reduce the IMD due to clipping from the weaker signal band. In this case, due to the nature of the clipping process, 3rd, 5th and 7th order operators are used in the reference generation, all being further weighted with separate two-tap adaptive filters and subtracted from the weak signal observation. Again LMS algorithm is used to control the adaptive filter parameters. The corresponding demodulated signal constellation of the weak signal is illustrated in Fig. 7, both without compensation (left part) and with compensation (right part). Clearly the post-processing is again able to reduce the distortion at the weak signal band in a considerable manner.

V. CONCLUSIONS

This article addressed the A/D converter nonlinear distortion with special emphasis on wideband radio receivers with high dynamic range for the digitized signal. Adaptive interference cancellation based digital post-processing was proposed to reduce the intermodulation distortion from the weak signal bands, stemming from either converter integral nonlinearity or input clipping (converter saturation), and originating from strong blocking signals. Both computer simulations and laboratory measurements based examples were used to demonstrate the applicability of the proposed post-processing, with commercially available A/D converters. The obtained results indicate that the observable signal-to-noise-and-distortion ratio (SNDR) at the weak signal bands can be considerably improved using the proposed technique. Future work will include more complete performance measurements and evaluations, and building a real-time prototype implementation using FPGA's.

REFERENCES

[1] P.-I. Mak, S.-P. U, and R. P. Martins, "Transceiver architecture selection: review, state-of-the-art survey and case study", *IEEE Circuits and Systems Mag.*, vol. 7, 2nd quarter 2007, pp. 6-25.

[2] A. Rusu, D. Rodriguez de Llera Gonzalez, and M. Ismail, "Reconfigurable ADCs enable smart radios for 4G wireless connectivity," *IEEE Circuits and Devices Mag.*, vol. 22, no. 3, pp. 6-11, May-June 2006.

[3] T. Araujo and R. Dinis, "Analytical evaluation and optimization of the ADC (analog-to-digital converter) in software radio architectures," in *Proc. IEEE Global Telecommun. Conf.* (GLOBECOM-04), Dallas, TX, USA, 2004, pp. 1066-1070, vol. 2.

[4] J. Yang, R. W. Brodersen and D. Tse, "Addressing the dynamic range problem in cognitive radios," in *Proc. IEEE Int. Conf. Communications* (ICC-07), pp. 5183-5188, June 24-28, 2007, Glasgow, Scotland.

[5] N. Vun, A.B. Premkumar, "ADC systems for SDR digital front-end," in *Proc. Int. Symp. Consumer Electronics* (ISCE-05), June 14-16, 2005, pp. 359–363.

[6] F. Maloberti, *Data Converters*. Dordrecht, The Netherlands: Springer, 2008.

[7] J. A. Wepman, "Analog-to-digital converters and their applications in radio receivers," *IEEE Commun. Mag.*, vol. 33, pp. 39-45, May 1995.

[8] R. H. Walden, "Analog-to-digital converter survey and analysis," *IEEE J. Selected Areas in Communications*, vol. 17, no. 4, pp. 539-550, April 1999.

[9] ITU-R, *Requirements Related to Technical Performance for IMT-Advanced Radio Interface(s)*, Report ITU-R M.2134, Dec. 2008. Available online at http://www.itu.int/.

[10] P. Arpaia, P. Daponte, and S. Rapuano, "A state of the art on ADC modeling," *Elsevier J. Comput. Standards & Interfaces*, vol. 26, pp. 31–42, Jan. 2004.

[11] D. Dardari, "Joint clip and quantization effects characterization in OFDM receivers," *IEEE Trans. Circuits Syst. I*, vol. 53, no. 8, Aug. 2006, pp. 1741–1748.

[12] L. Michaeli, P. Michalko, and J. Saliga, "Unified ADC nonlinearity error model for SAR ADC," *Elsevier J. Measurement*, vol. 41, pp. 198–204, Feb. 2008.

[13] IEEE-SA Standards Board, *IEEE Standard for Terminology and Test Methods for Analog-to-Digital Converters*, IEEE Std #1241-2000, June 2001.

[14] M. Allén, J. Marttila and M. Valkama, "Modeling and mitigation of nonlinear distortion in wideband A/D converters for cognitive radio receivers," in preparation.

[15] M. Valkama, A. Shahed, L. Anttila, and M. Renfors, "Advanced digital signal processing techniques for compensation of nonlinear distortion in wideband multicarrier radio receivers," *IEEE Trans. Microwave Theory and Techniques*, vol. 54, pp. 2356-2366, June 2006.

[16] E. Keehr and A. Hajimiri, "Equalization of IM3 products in wideband direct-conversion receivers," *IEEE J. Solid-State Circuits*, vol. 43, pp. 2853-2867, Dec. 2008.

[17] Analog Devices, *AD9218 Data Sheet*, rev. C, Dec. 2006. Available online at http://www.analog.com/

[18] Analog Devices, "How ADIsimADC models an ADC," application note AN-737, rev. B, 2009. Available online at http://www.analog.com/

[19] Analog Devices, *AD9248 Data Sheet*, rev. A, March 2005. Available online at http://www.analog.com/

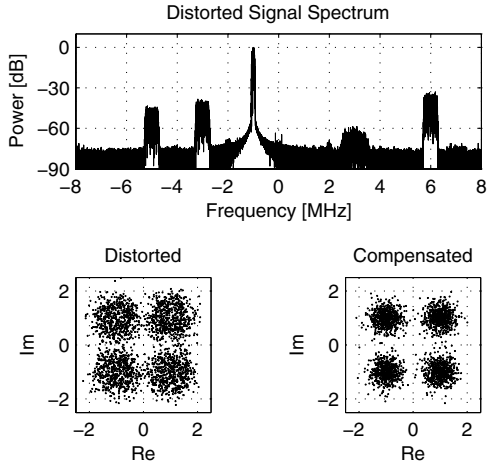

Fig. 5. Upper part: Spectrum of the received signal with 5 frequency channels and 60 dB dynamic range, 10-bit A/D converter. Lower part: Demodulated signal constellations of the weak QPSK signal at 3 MHz without and with post-processing.

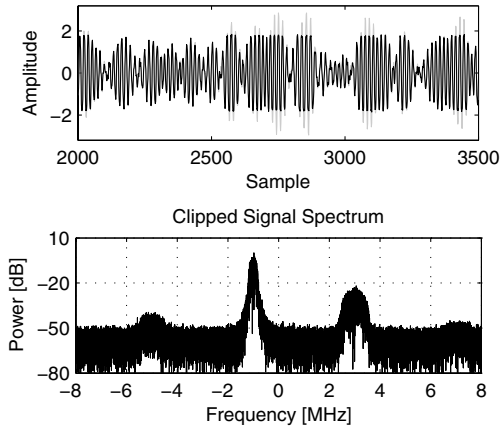

Fig. 6. Upper part: Measured time-domain digitized waveform under clipping (black) and the corresponding ideal unclipped waveform (gray). Lower part: Spectrum of the measured waveform under clipping. Third-order IMD of the stronger signal at -1 MHz is masking the weaker signal at 3 MHz. 14-bit A/D converter was used.

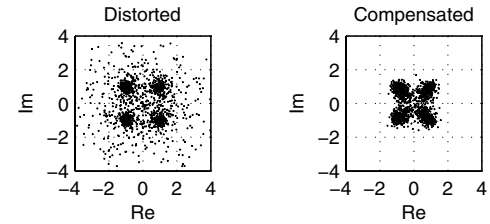

Fig. 7. Measured demodulated signal constellations of the weak QPSK signal at 3 MHz without and with post-processing under clipping.